JGR Atmospheres

RESEARCH ARTICLE
10.1029/2020JD032793

Key Points:
- Evidence for direct convective hydration of the lower stratosphere is assessed with in situ and remote sensing measurements
- Direct convective hydration of the extratropical lower stratosphere occurs primarily over North America during summertime
- Direct convective hydration of the tropical lower stratosphere is rare and limited to slight enhancements just above the tropopause

Correspondence to:
E. J. Jensen,
ericjj50@gmail.com

Citation:
Jensen, E. J., Pan, L. L., Honomichl, S., Diskin, G. S., Krämer, M., & Spelten, N., et al. (2020). Assessment of observational evidence for direct convective hydration of the lower stratosphere. *Journal of Geophysical Research: Atmospheres*, *125*, e2020JD032793. https://doi.org/10.1029/2020JD032793

Received 23 MAR 2020
Accepted 16 JUN 2020
Accepted article online 23 JUN 2020

Assessment of Observational Evidence for Direct Convective Hydration of the Lower Stratosphere

E. J. Jensen[1], Laura L. Pan[1], Shawn Honomichl[1], Glenn S. Diskin[2], Martina Krämer[3,4], Nicole Spelten[3], Gebhard Günther[3], Dale F. Hurst[5,6], Masatomo Fujiwara[7], Holger Vömel[1], Henry B. Selkirk[8], Junko Suzuki[9], Michael J. Schwartz[10], and Jessica B. Smith[11]

[1]Atmospheric Chemistry Observations and Modeling Laboratory, National Center for Atmospheric Research, Boulder, CO, USA, [2]NASA Langley research Center, Hampton, VA, USA, [3]Research Center Jülich, Institute for Energy and Climate Research-7, Jülich, Germany, [4]Institute for Physics of the Atmosphere, Johannes Gutenberg University of Mainz, Mainz, Germany, [5]Cooperative Institute for Research in Environmental Sciences, University of Colorado Boulder, Boulder, CO, USA, [6]Global Monitoring Division, NOAA Earth System Research Laboratory, Boulder, CO, USA, [7]Graduate School of Environmental Science, Hokkaido University, Sapporo, Japan, [8]Goddard Earth Sciences and Technology Center, University of Maryland, Baltimore County, Baltimore, MD, USA, [9]Japan Agency for Marine-Earth Science and Technology, Yokosuka, Japan, [10]Jet Propulsion Laboratory, California Institute of Technology, Pasadena, CA, USA, [11]Harvard John A. Paulson School of Engineering and Applied Sciences, Harvard University, Cambridge, MA, USA

Abstract In situ and remote sensing observations of water vapor are analyzed to assess the evidence for direct convective hydration of the lower stratosphere. We have examined several hundred balloon-borne and airborne in situ measurements of lower stratospheric humidity in the tropics and northern midlatitudes. We find that the tropical lower stratospheric H_2O enhancements above the background occur quite infrequently, and the height of the enhancements is within about 1 km of the cold-point tropopause. Following Schwartz et al. (2013, https://doi.org/10.1002/grl.50421), we examine the anomalously high (above 8 ppmv) water vapor mixing ratios retrieved by the Aura Microwave Limb Sounder (MLS) at 100- and 82-hPa pressure levels, and we determine their vertical location relative to the local tropopause based on both Global Forecast System (GFS) operational analysis and the ERA5 reanalysis temperature data. We find that essentially all of the >8-ppmv MLS water vapor measurements over the extratropical North American monsoon region are above the relatively low lapse-rate tropopause in the region, and most are above the local cold-point tropopause. Over the Asian monsoon region, most (80/90%) of the high H_2O values occur below the relatively high-altitude local lapse-rate/cold-point tropopause. Anomalously high MLS water vapor retrievals at 100 and 82 hPa almost never occur in the deep tropics. We show that this result is consistent with the in situ observations given the broad vertical averaging kernel of the MLS measurement. The available evidence suggests that direct hydration of the lower stratosphere is important over North America during the monsoon season but likely has limited impact in the tropics.

1. Introduction

Recognition of the importance of stratospheric humidity for the Earth's climate (Forster & Shine, 2002; Solomon et al., 2010) has prompted extensive research over the past few decades focused on understanding the processes controlling stratospheric water vapor and understanding the causes of observed stratospheric humidity variations. Since air primarily enters the stratosphere across the tropical tropopause and the Brewer-Dobson circulation transports this air throughout the stratosphere, the key issue is what controls humidity of air entering the stratosphere across the tropical tropopause (H_2O_{entry}). (Methane oxidation in the middle and upper stratosphere also contributes to stratospheric humidity, but this source term is well characterized.)

Extensive evidence points to the dominance of temperature control in explaining the subseasonal, seasonal, and interannual variability of stratospheric humidity (Mote et al., 1996; Randel & Park, 2019; Randel et al., 2004). The physics behind the temperature-humidity correlation involves freeze drying of air as it ascends across the cold tropical tropopause: Vapor in excess of ice saturation is removed by growing

and sedimenting ice crystals. Accurate calculation of H_2O_{entry} requires detailed treatment of cloud processes such as ice nucleation, deposition growth, and sedimentation, as well as small-scale gravity wave-driven temperature fluctuations (Jensen & Pfister, 2004; Schoeberl et al., 2016; Ueyama et al., 2015, 2018), but the temporal variability of H_2O_{entry} seems to be largely controlled by temperature variability. It is important to note that convection detraining in the upper troposphere has a dominant impact on the horizontal distribution of tropospheric water vapor at 100 hPa during boreal summertime (Ueyama et al., 2018); the impact of deep convection detraining directly into the lower stratosphere remains an open question.

A potentially important source of water vapor from extreme deep convection detraining ice directly into the lowermost stratosphere has been hypothesized for decades (Adler & Mack, 1986; Danielsen, 1993), and the potential importance of this source continues to be suggested in recent studies (Avery et al., 2017; Dessler et al., 2016; Wang et al., 2019). It is useful to distinguish here between direct and indirect convective influence on stratospheric humidity. The direct pathway involves deep convection extending above the local cold-point tropopause (CPT) and the irreversible mixing of saturated air laden with ice crystals into the lowermost stratosphere. When convection extends significantly above the cold point into warmer, very dry air in the lower stratosphere, there is a strong potential for hydration (Schoeberl et al., 2018; Smith et al., 2017). Convective hydration can increase the lower stratospheric H_2O mixing ratio up to the local saturation mixing ratio. Taking a typical temperature gradient just above the tropical tropopause of $+6$ K km^{-1} and a representative cold point temperature of 190 K and pressure of 90 hPa with a corresponding saturation H_2O mixing ratio of 3.6 ppmv, the saturation mixing ratios 1 and 2 km above the tropopause are about 10 and 25 ppmv, respectively.

The indirect effect of deep convection on stratospheric humidity involves detrainment of ice into the tropical uppermost troposphere, followed by ascent into the stratosphere. Above about 15 km in the tropics, air is slowly ascending in balance with radiative heating as part of the Brewer-Dobson circulation (Yang et al., 2010). If a convectively influenced air parcel between 15 km and the tropical tropopause does not encounter supersaturation with respect to ice, cirrus formation, and dehydration on its subsequent journey upward into the stratosphere, then the convective influence in the uppermost troposphere will affect stratospheric humidity. If the air parcel encounters temperatures cold enough for in situ cirrus formation, then the impact of convective influence can be partially lost. Trajectory analysis shows that in most cases, the final influence on the humidity of air parcels entering the tropical stratosphere is dehydration by in situ cloud formation (Schoeberl et al., 2018; Ueyama et al., 2015, 2018). Note also that convection can both hydrate and dehydrate the tropical uppermost troposphere (Jensen et al., 2007; Schoeberl et al., 2018; Ueyama et al., 2015; 2018). If convection detrains saturated air and ice into ambient supersaturated air (which is common in the tropical uppermost troposphere), then the humidity will be drawn down toward saturation. When convective detrainment into subsaturated air occurs, the result will be hydration. Since the relative humidity in the stratosphere is quite low, the direct impact of convection reaching the lower stratosphere will always be hydration.

Even when overshooting deep convection extends into the lowermost stratosphere, irreversible transport of air and ice into the stratosphere is not guaranteed. The overshooting air mass may simply relax back into the troposphere with a time scale on the order of the Brunt-Väisälä period ($\simeq$15 min). Cloud-resolving model studies of overshooting convection have shown that both turbulent mixing and breaking gravity waves play important roles in driving irreversible mixing between convective overshoots and environmental stratospheric air (Dauhut et al., 2018; Hassim & Lane, 2010; Homeyer et al., 2017; Wang, 2003). From a practical perspective, the large uncertainty in the mass of irreversibly transported air for each convective system limits the accuracy of modeling studies estimating the regional and global impact of overshooting convection based on satellite measurements of convective cloud-top heights.

Here, we focus on direct evidence of convective hydration of the lower stratosphere from measurements of water vapor. A number of previous studies have documented water vapor measurements clearly indicating convective hydration in the lowermost stratosphere. The most compelling evidence comes from in situ measurements in the lower stratosphere over the midlatitude North American monsoon (NAM) region. Smith et al. (2017) showed aircraft measurements indicating layers of enhanced humidity (water vapor mixing ratios on the order of 12 ppmv in a region where the background lower stratospheric humidity is $\simeq$6

ppmv) at potential temperatures as high as about 410 K over north America during Boreal summertime. Trajectory analysis showed that these enhanced H_2O layers were associated with overshooting convection extending well above the local tropopause. The NAM region is also where many of the highest outliers in the Aura Microwave Limb Sounder (MLS) H_2O observations at 100 and 82 hPa occur (Schwartz et al., 2013). It seems likely that the observed local maximum of summertime 100-hPa water vapor in the NAM region indicated by satellite measurements can be attributed to convective hydration in the region. The impact of north American convection on zonal mean or global stratospheric humidity budgets is less clear.

Layers with enhanced humidity in the lowermost stratosphere have also been observed with in situ measurements in the deep tropics (Corti et al., 2008; Kley et al., 1982, 1993; Schiller et al., 2009). However, as shown below, these hydration layers are generally not far above the local CPT (within 1–2 km), and the water vapor mixing ratios in the layers are no more than 1–2 ppmv above the background value. Three of these cases were associated with the well-documented intense "Hector" thunderstorm that occurs during the premonsoon and monsoon break periods over the Tiwi Islands north of Darwin Australia (Connolly et al., 2013; Dauhut et al., 2018).

In this paper, we investigate the occurrence of convectively enhanced water vapor in the lower stratosphere using a combination of in situ and remote sensing measurements. We analyze aircraft and balloon measurements of UTLS water vapor in the tropics, and we reanalyze the MLS H_2O observations of enhanced water vapor in tropopause relative coordinates for both tropical and midlatitude regions. We additionally assess the constraint placed on convective hydration of the lowermost stratosphere by MLS measurements given the ≃3-km vertical resolution.

2. Data Products

2.1. High-Altitude Aircraft In Situ H_2O Measurements

High-altitude aircraft are required for in situ sampling the tropical upper troposphere/lower stratosphere (UTLS) region. As noted above, aircraft measurements of enhanced-H_2O plumes over North America during boreal summertime have been documented by (Smith et al., 2017) (and references therein). Here, we use measurements in the deep tropics made with the National Aeronautics and Space Administration (NASA) Global Hawk during the ATTREX campaign (Jensen et al., 2017) and the WB-57 aircraft during the POSIDON campaign. Both campaigns extensively sampled the western Pacific Tropical tropopause layer (TTL, ~13-18 km) in the tropical western Pacific (see Figure 1). Temperature and water vapor were measured with the Meteorological Measurement System (MMS) and the Diode Laser Hygrometer (DLH), respectively. DLH provides excellent precision even under dry UTLS conditions (50 ppbv for a 20-Hz data rate). The flights from these campaigns spanned the tropical western Pacific region during February–March 2014 (ATTREX) and October 2016 (POSIDON). Deep convection was prevalent during both of these campaigns, although during ATTREX, the flight planning generally avoided sampling in close proximity to active convection. POSIDON included three flights near an active typhoon.

The primary sampling strategy used in these campaigns was to repeatedly ascend and descend through the UTLS region. The maximum altitude achievable with the Global Hawk was only above the tropopause near the ends of the long-duration flights after most of the fuel had burned off. We use only the 18 profiles that extended at least 1 km above the CPT. During POSIDON some of the aircraft ascents were deliberately cut short before the WB-57 aircraft had ascended well into the lower stratosphere. These decisions were driven by a tradeoff between flight time required for the aircraft to slowly ascend all the way to maximum altitude and the relative value of sampling within the upper troposphere compared to the lower stratosphere. Here, we use only the 63 POSIDON vertical profiles that extended at least 1 km above the local CPT.

We additionally use water vapor measurements made in the tropical UTLS with instruments onboard the Russian M55 Geophysica high-altitude aircraft during multiple tropical campaigns. Total water (vapor + ice) was measured with the Fast In Situ Stratospheric Hygrometer (FISH), which uses a Lyman-α photofragment fluorescence technique (Meyer et al., 2015; Zöger et al., 1999). We include data from three tropical campaigns: The Tropical Convection, Cirrus and Nitrogen Oxide experiment (TroCCiNOx) in January and February 2005 from Aracatuba, Brazil; the Stratospheric-Climate Links with Emphasis on the Upper Troposphere and Lower Stratosphere (SCOUT-O3) in November and December 2005 from Darwin,

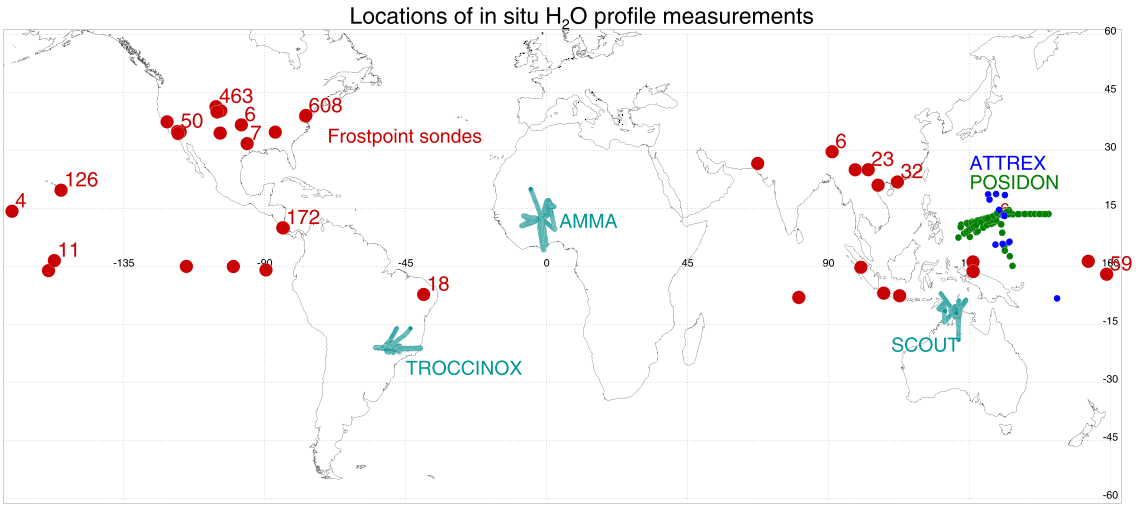

Figure 1. Locations of in situ water vapor profile measurements. Frost point sondes are indicated by red circles, with numbers indicating the total number of sonde profiles for each location. Blue dots show locations of ATTREX Global Hawk vertical profiles extending at least 1 km above the local CPT, and green dots show the locations of POSIDON WB-57 profiles extending into the stratosphere. The Geophysica campaign flight tracks (cyan) are also shown.

Australia; and the African Monsoon Multidisciplinary Analysis (AMMA/SCOUT-O3) experiment in August 2006 from Ouagadougou, Burkina Faso. All three campaigns occurred in locations and seasons with strong continental deep convection.

2.2. Frost-Point Balloon Soundings

Frost point hygrometers (FPs) measure atmospheric water vapor in situ using the chilled mirror principle. The first FP for high-altitude airborne measurements was developed by Brewer (1949). When deployed on meteorological balloons, modern FPs provide water vapor vertical profiles from the surface to the middle stratosphere with a vertical resolution better than 100 m and an accuracy of 6–10% (Hall et al., 2016; Vömel et al., 2016). FPs have been launched at numerous locations over the last four decades (Figure 1), mostly for short-term measurement campaigns or seasonal studies. The field campaign projects include the Soundings of Ozone and Water in the Equatorial Region (SOWER) project at sites in Indonesia, Vietnam, Kiribati, and Ecuador (Fujiwara et al., 2010; Hasebe et al., 2013), the Ticosonde project at San Jose in Costa Rica (Fujiwara et al., 2010; Selkirk et al., 2010), the Sounding Water vapor, Ozone and Particle (SWOP) project at sites in China except for Yangjiang (Bian et al., 2012), the 8th World Meteorological Organization (WMO) Intercomparison of High Quality Radiosonde Systems in Yanjiang, China (Nash et al., 2011), and the research vessel Mirai campaign in the tropical Indian Ocean (Suzuki et al., 2013). Only a handful of sites (such as Boulder, CO, and Hilo, HI) have maintained year-around FP launches to compile climate records of UTLS water vapor that span a decade or more (Fujiwara et al., 2010; Hurst et al., 2011). The Ticosonde launches from Costa Rica also include multiple years and seasons for analysis of inter-annual and seasonal variability (Schoeberl et al., 2019).

2.3. MLS H_2O

The satellite measurement of water vapor used here comes from the MLS on board the Aura satellite. We use the Version 4.2 water vapor retrieval (Read et al., 2007). With approximately 3,500 scans of the earth's limb each day and 100-hPa H_2O precision and accuracy of 15% and 8%, respectively, MLS provides the necessary sampling statistics and accuracy required for observing the anomalous enhancements in lower stratospheric humidity caused by overshooting convection (Schwartz et al., 2013). The MLS vertical resolution in the tropopause region is about 3 km, and the horizontal footprint is about 200 km along track by 7 km cross track. For the anomalously high water vapor events that are mostly within 1–2 km of the local tropopause, the averaging kernel will partially straddle the tropopause, resulting in contributions to the retrieved H_2O from both the upper troposphere and lower stratosphere. We return to this issue in section 4.

2.4. Meteorological Analyses

For determination of the local tropopause height corresponding to the MLS H_2O observations, we use the National Centers for Environmental Prediction (NCEP) Global Forecast System (GFS) operational analysis (Pan & Munchak, 2011) and the ERA5 reanalysis (Hoffmann et al., 2019). The ERA5 data product is the successor of the well-known ERA Interim reanalysis and replaces it since September 2019. The major improvements of ERA5 over ERA Interim include much higher spatial (0.25 × 0.25°) and temporal (hourly) resolution. Most important for this study, the ERA5 reanalysis model has 29 vertical levels between 300 and 50 hPa.

We use both the lapse-rate tropopause (LRT) based on the WMO definition of 2-K km^{-1} temperature gradient threshold and the CPT defined simply as the vertical location of the temperature minimum. Pan and Munchak (2011) compared the GFS LRT with coincident radiosonde temperature profiles and estimated the one standard deviation uncertainty in GFS LRT to be about 650 m. For the ERA5 reanalysis, we calculate both the LRT and CPT using the native model grid resolution of about 300 m near the tropopause. Tegtmeier et al. (2020) showed improved accuracy of the LRT and CPT in ERA5 compared to previous reanalyses. Their comparison with radiosondes also showed that the zonal mean tropopause height is within about 200 m of the radiosonde value.

3. Stratospheric H_2O Outliers Indicated by In Situ Measurements

As noted above, high-altitude aircraft campaigns have provided numerous UTLS vertical profiles with accurate measurements of temperature and water vapor. We begin by examining recent aircraft measurements in the deep tropics. For this analysis, we only include the profiles that extend at least 1 km above the CPT (18 profiles from ATTREX and 63 profiles from POSIDON).

In many of the POSIDON ascents/descents, there was a minimum in the water vapor profile near the cold point associated with recent dehydration as the tropopause temperature decreased in boreal autumn. The lower stratospheric "background" water vapor mixing ratio of about 4.5–6 ppmv was associated with air that ascended across the relatively warm tropopause during the previous boreal summer, and recent dehydration near the colder western Pacific tropopause during October decreased the water vapor mixing ratio near the tropopause to about 2–3 ppmv. Given this water vapor structure, only layers with H_2O above the background value of 5–6 ppmv could unambiguously be attributed to direct convective hydration.

Of the 81 ATTREX and POSIDON UTLS profiles, only one case of apparent convective hydration was found. Figure 2 shows the height profiles of temperature, water vapor, and ozone for this example on the flight of 15 October 2016. Ozone was measured with the NOAA dual-beam ultraviolet (UV) absorption photometer (Gao et al., 2012). A distinct layer is evident at ≃17.5 km with a peak H_2O mixing ratio about 1.5 ppmv above the background. The layer was only about 0.5 km above the local CPT. The ozone mixing ratio at the height of the enhanced-H_2O layer was about 150 ppbv, indicating a mixture of tropospheric and stratospheric air. Note that this flight was sampling convectively generated cirrus along the edges of Typhoon Haima. Two additional flights on 18 and 19 October sampled along the outskirts of the typhoon, but no further indication of direct stratospheric hydration was evident.

We have additionally examined the 31 water vapor profiles from Geophysica flights in the deep tropics. All of these flights were in the vicinity of strong continental convective systems. As shown by Corti et al. (2008) and Schiller et al. (2009), a few of these flights indicated enhancements in water vapor above the local CPT. Some of the profiles also indicated ice crystals above the tropopause, indicating a potential for hydration if the ice crystals were to sublimate before falling below the tropopause. The clearest example from the Geophysica campaigns is the profile near the Hector thunderstorm documented by Corti et al. (2008). We have replotted the water vapor profile using geometric height as the vertical coordinate in Figure 2. As with the POSIDON example, the water vapor enhancements were no larger than about 1–2 ppmv, and the hydrated layers were no more than about 1 km above the tropopause.

The database of frost point soundings includes several hundred profiles over North America, 172 profiles over San Jose, Costa Rica, a small number of soundings across the Pacific near the equator, a small number of soundings in the Maritime Continent region, and a few dozen soundings over China (Figure 1). The monthly frost point soundings over Boulder, Colorado (40.0°N, 105.3°E), provide a long timeline of high-quality water

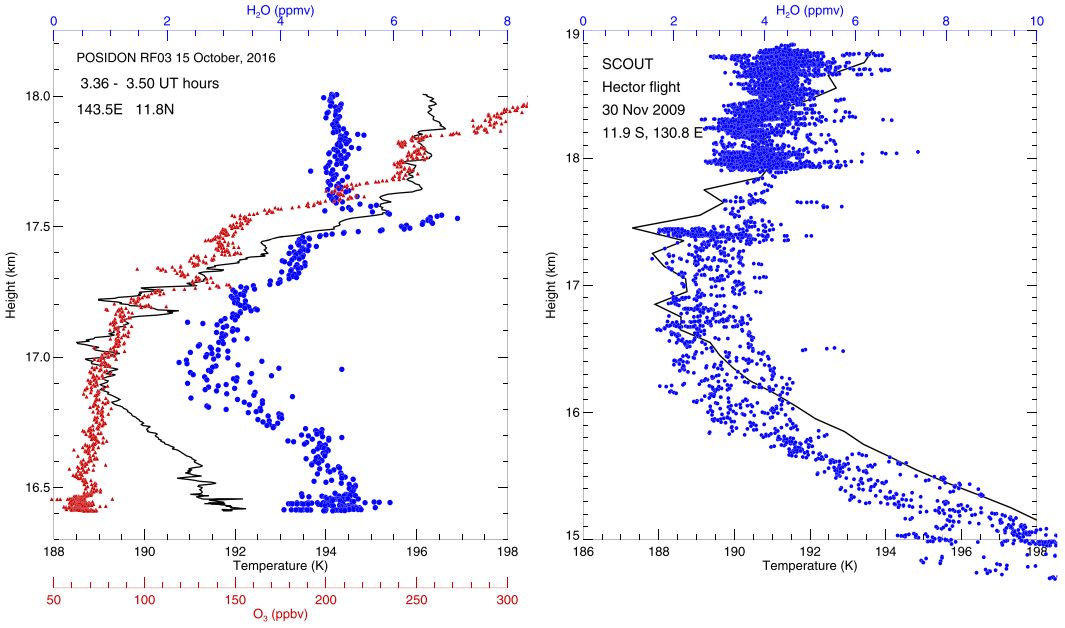

Figure 2. (left panel) Vertical profiles of temperature (black), H_2O mixing ratio (blue), and ozone mixing ratio (red) are shown from a vertical profile on 15 October 2016 when the WB-57 aircraft was sampling anvil cirrus on the outskirts of Typhoon Haima. The layer of enhanced H_2O concentration at 17.5 km (about 0.5 km above the local CPT) was likely caused by direct convective hydration. (right panel) Water vapor profile from the Scout-O3 Geophysica flight near the Hector thunderstorm.

vapor profiles. None of these Boulder soundings indicates clear evidence of lower stratospheric hydration; however, the location is west of where most of the stratosphere-penetrating convective systems seem to occur (Smith et al., 2017). Thus, the lack of evidence for lower stratospheric hydration in the Boulder frost point soundings is not necessarily inconsistent with the aircraft measurements indicating convective hydration of the lower stratosphere during the NAM. The Costa Rica soundings were relatively near the Panama Bight and northern Columbia where some of the strongest deep convection occurs during boreal summertime (Liu & Liu, 2016; Zipser et al., 2006). The lack of evidence for lower stratospheric hydration in the summertime Costa Rica H_2O profiles could indicates either a lack of lower stratospheric hydration by the nearby convection or prevailing winds advecting the hydrated air away from San Jose. As shown by Bian et al. (2012), the frost point soundings over China during the monsoon season indicate saturation with respect to ice up to the CPT but no evidence of convective hydration above the relatively high Asian monsoon (ASM) region tropopause. In summary, neither the tropical or northern midlatitude frost point soundings provide clear evidence of direct convective hydration of the lower stratosphere.

4. Stratospheric H_2O Outliers in Satellite Measurements

As discussed above, Schwartz et al. (2013) identified all anomalously high (above 8 ppmv) MLS water vapor retrievals at the 100- and 82-hPa pressure levels. Their analysis included the first 8 years of MLS data. The vast majority of these events occurred over the Asian and NAM regions during June, July, and August (see Schwartz et al., 2013, Figure 2). We have used the same approach to identify the 100- and 82-hPa H_2O outliers including all MLS data through the summer of 2019. As discussed by Schwartz et al. (2013), nearly all of these events occur at 100 hPa, with only a handful at 82 hPa. For determination of the height of these events relative to the local tropopause, we calculate the local GFS LRT and the ERA5 LRT and CPT at the locations and times corresponding to each high MLS H_2O event. We further calculate the pressure altitude corresponding to the LRT and CPT pressures for comparison with the pressure altitude corresponding to the MLS measurement level. Figure 3 shows the locations of MLS 100- and 82-hPa H_2O retrievals above 8 ppmv, with the symbols color coded to indicate the difference between the MLS level pressure altitude and the GFS LRT pressure altitude. In agreement with Schwartz et al. (2013), we find that most

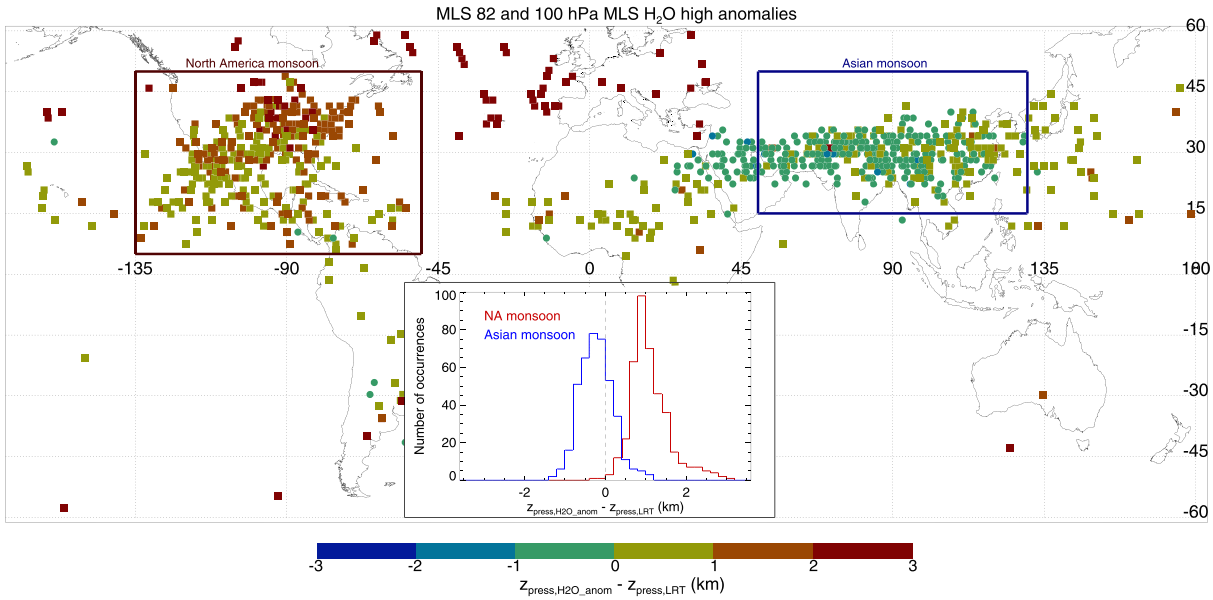

Figure 3. The locations of anomalously high (>8 ppmv) 100- and 82-hPa MLS water vapor measurements are indicated by color symbols on the map. The symbol colors indicate the difference between the MLS level pressure altitude and the LRT pressure altitude. Events for which the MLS level is above the LRT are indicated by squares, and events for which the MLS level is below the LRT are indicated by circles. The inset figure shows frequency distributions of the difference between the MLS level pressure altitude and the local LRT pressure altitude with red and blue curves corresponding to the NAM and ASM monsoon regions indicated by the red and blue boxes on the map. All of the NAM high-H_2O events are above the local LRT, whereas most of the ASM events are below the local LRT.

of the anomalously high MLS water vapor mixing ratio values occur above the NAM and ASM regions during boreal summertime. There are a few occurrences over the central Pacific and central Africa that might be associated with extreme convective events. Note that if we included all months in our analysis, Figure 3 would essentially be unchanged since there are only a handful of high water vapor anomaly events outside the months of June, July, and August.

Frequency distributions of pressure-altitude difference between the MLS level and the GFS LRT for the NAM and ASM regions indicated by the red and blue boxes are shown in the Figure 3 inset. Perhaps surprisingly, essentially *all* of the NAM high-H_2O events are above the local GFS LRT, whereas most of the ASM events are below the local LRT, with a tail of infrequent events above the LRT. Since the uncertainty in analysis-model tropopause determination is several hundred meters, it is possible that some of the ASM humid layers that appear to be above the local tropopause are caused by errors in the tropopause determination (or vice versa).

Locations of the anomalously high MLS retrievals relative to the local tropopause are further examined using the ERA5 temperature fields. Figure 4 shows frequency distributions of ERA5 tropopause pressure and the pressure altitude difference between the anomalous MLS retrievals and the local ERA5 LRT and cold-point tropopause. The data are subsetted into the NAM and ASM regions. The temperature structure is quite different for the two monsoon regions, with typical midlatitude tropopause pressures (≃120–100 hPa) over the NAM region and very high tropopause heights (≃100–75 hPa) over the ASM region. The pressure altitude difference frequency distributions (bottom panel of Figure 4) show that the majority of anomalous MLS retrievals over the NAM are above the ERA5 CPT, whereas very few of the anomalous MLS retrievals over the ASM are above the ERA5 CPT.

The water vapor concentration in the lowermost tropical stratosphere has a seasonal variation corresponding to the seasonal variation in tropical tropopause temperature (Mote et al., 1996). Prevailing lower stratospheric H_2O mixing ratios are about 4.5–6 ppmv in the Boreal summertime and 2- to 3-ppmv range during wintertime. Therefore, a lower threshold H_2O mixing ratio for identification of high anomalies can be used during boreal wintertime than the 8-ppmv value chosen above. Also, the wintertime tropopause is higher

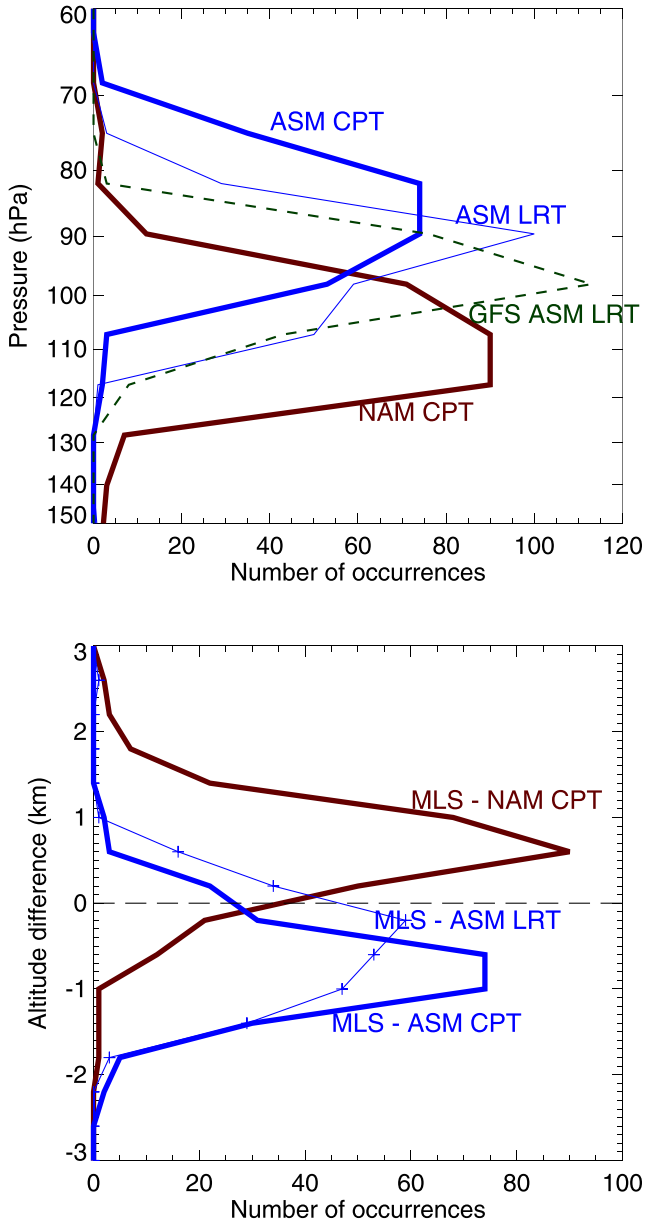

Figure 4. (top panel) Frequency distributions of cold-point and lapse-rate tropopause pressure over the North American and Asian monsoon regions from ERA5 are shown. The green dashed curve shows the height distribution of the GFS lapse-rate tropopause over the Asian monsoon for comparison. The GFS and ERA5 lapse-rate tropopause pressures are in good agreement. (bottom panel) Pressure altitude differences between the anomalous MLS retrieval pressures (mostly 100 hPa) and the corresponding tropopause pressure altitudes determined from ERA5 fields.

than during summer, such that 100 hPa is typically below the tropopause. Using a threshold value of 6 ppmv for high H_2O anomalies at 82 hPa, we find only seven occurrences during December, January, and February. Five of these cases are over South America, possibly caused by the strong convection east of the Andes (Schwartz et al., 2013; Zipser et al., 2006). We do not find any wintertime 82-hPa H_2O retrievals in the MLS record above 6 ppmv in other regions with strong convection, such as southern Africa or the Maritime Continent (Liu & Zipser, 2005).

The broad MLS vertical averaging kernel (≃3 km) limits the ability to detect narrow layers with high humidity. As a demonstration of the importance of this limitation, we have constructed water vapor profiles based on the POSIDON example shown in Figure 2 with variations in the magnitude of the H_2O enhancement in the layer near 17.5 km (see Figure 5). As an upper limit, we further assume that the enhanced water vapor layer occupies the entire MLS horizontal footprint (200 × 7 km); in reality, the convective water vapor plumes will likely occupy only a fraction of this footprint. Convective water vapor plumes would presumably only occupy a large horizontal area after they had sufficient time to disperse. The corresponding H_2O values obtained by convolving the humidity profiles with the MLS 82- and 100-hPa averaging kernels and a prioris are shown in the Figure 5 legend. Significant increases in the MLS-retrieved water vapor concentrations only occur if the layer H_2O mixing ratio is greater than 10 ppmv. However, such high mixing ratios would exceed the saturation mixing ratio corresponding to the temperature in the layer (black dashed curve in Figure 2). This example shows that, within the constraint of the local saturation mixing ratio, narrow humid layers in the tropical lower stratosphere would not necessarily produce MLS retrievals significantly above the 6- to 8-ppmv background. Therefore, the lack of anomalously high MLS H_2O retrievals above the tropopause in the deep tropics is not inconsistent with the in situ measurements indicating that narrow lower stratospheric enhanced H_2O layers do occasionally occur.

One can envision an extreme scenario in which convection generates a water vapor mixing ratio profile corresponding to the H_2O saturation mixing ratio all the way up to the convective cloud top. An extensive anvil cirrus cloud with cloud top above the tropopause could possibly produce such a water vapor profile, and the plume could conceivably fill the horizontal MLS footprint. We note these assumptions are likely unrealistic since convective overshoots are typically quite localized (Bedka & Khlopenkov, 2016), and observations of lower stratospheric water vapor enhancements indicate that they typically occur in narrow layers. Nonetheless, this scenario represents the maximum possible impact of convection on the local lower stratospheric humidity profile. Recent in situ measurements in active convection near the tropopause indicate substantial supersaturation with respect to ice (Krämer, 2020), which would imply even higher H_2O mixing ratios than we assume here. However, it seems likely that once the convective vertical motions settle down, the water vapor mixing ratio should approach ice saturation within the anvils. In order to evaluate the implications of such humid regions for MLS H_2O retrievals, we have constructed water vapor profiles using high-resolution radiosonde temperature profiles from Guam (13.5°N). For each temperature profile, we use the saturation mixing ratio up to an assumed convective cloud top pressure, and we use 3-ppmv H_2O above the convective cloud top. Frequency distributions of 82-hPa MLS H_2O retrievals calculated with these water vapor profiles for boreal winter and summer 2008 are shown in Figure 6. During boreal wintertime, the tropopause region is cold enough to

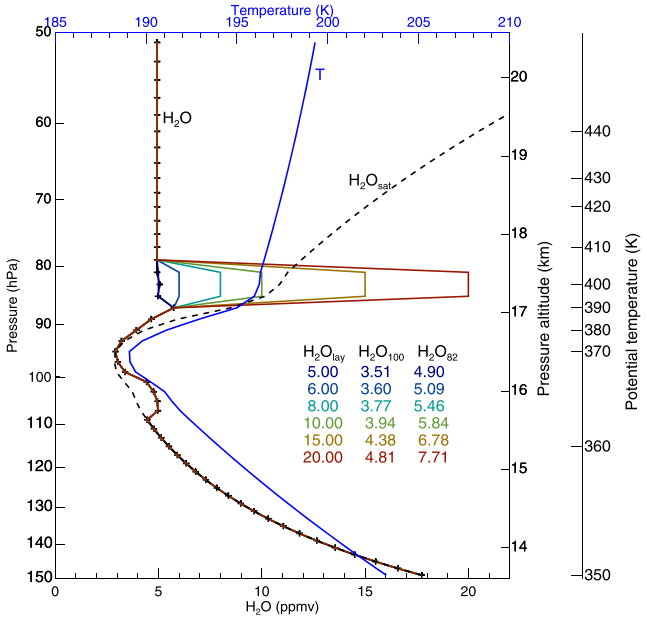

Figure 5. The impact of an enhanced-H_2O layer just above the CPT on MLS-retrieved water vapor at 82 and 100 hPa is shown. We construct water vapor profiles based on the POSIDON profile with an apparent convectively hydrated layer at about 17.5 km (Figure 2). The H_2O mixing ratio in the enhanced-H_2O layer is varied between 5 ppmv (the background value) and 20 ppmv (colored curves). The corresponding H_2O mixing ratios retrieved by MLS at 82 and 100 hPa are shown in the legend. The saturation mixing ratio profile (dashed black curve) corresponding to the temperature profile (blue curve) is also shown.

prevent MLS 82-hPa retrievals higher than about 4 ppmv when the convective cloud top height is below about 82 hPa. With the convective cloud top at 67 hPa, the 82-hPa retrieved H_2O values show a broader distribution, with a few values exceeding 6 ppmv. Given that these high values are rare even given the extreme assumptions of saturation up to cloud top and horizontal uniformity, it is not surprising that Boreal wintertime MLS 82-hPa retrievals above 6 ppmv do not occur in the tropics. Conversely, we conclude that the absence of Boreal wintertime MLS 82-hPa retrievals above 6 ppmv indicates that the water vapor enhancement scenario above 82 hPa hypothesized here does not occur.

During boreal summertime, the tropical tropopause is lower than in the winter, and convection up to even 91 or 82 hPa extends into relatively warm temperatures in the lower stratosphere. As a result, using the saturation mixing ratio up to 82 hPa in the constructed profiles results in MLS 82-hPa H_2O retrievals of several ppmv or higher. Such high values are never seen in the boreal summertime tropical 82-hPa MLS H_2O retrievals. With a convective cloud-top pressure of 100 hPa, the retrieved H_2O values at 82 hPa are all less than 6 ppmv, in agreement with the observations. Similar results are obtained if we use the 100-hPa MLS H_2O retrieval. This analysis suggests that either summertime tropical convective cloud tops never extend above about 90 hPa, or (more likely) convective overshoots extending above 90 hPa hydrate only a small fraction of the MLS sample volume.

5. Summary and Discussion

The results presented here, along with previous analyses of in situ and remote sensing water vapor measurements, suggest that direct convective hydration of the lower stratosphere primarily occurs in the extratropics over North America during the summertime monsoon season. Within the uncertainties in determination of tropopause height from analysis and reanalysis models, direct convective hydration of the lower stratosphere does not seem to occur over the ASM, primarily because the tropopause is very high there. These results are consistent with satellite measurements of water isotopes indicating enrichment of HDO in the lower stratosphere over the NAM, but no HDO enrichment over the ASM (Randel et al., 2012). The observations also indicate that direct convective hydration in the deep tropics is not occurring routinely at any time of the year.

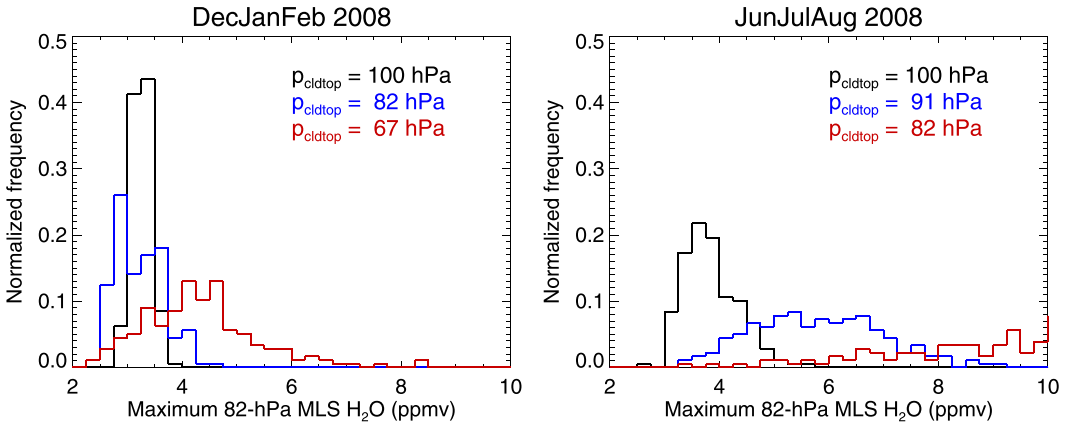

Figure 6. Frequency distributions of the maximum possible MLS-retrieved H_2O at 82 hPa corresponding to H_2O profiles with ice saturation up to convective cloud-top pressures indicated in the legend. Note that different convective cloud-top pressures are used for the wintertime (left panel) and summertime (right panel) calculations.

Of the hundreds of tropical H_2O profiles made with in situ instruments, only a few indicate convective enhancement above the local CPT, and even in these cases, the enhancements are modest (1–2 ppmv above background in layers with thickness less than 1 km), and they occur within 1 km of the CPT. Furthermore, these anecdotes of convective hydration in the tropics come from aircraft flights deliberately sampling the outflow from strong convective systems. Overall, the in situ measurements indicate that direct convective hydration just above the tropical tropopause does occur, but it is quite rare and the water vapor enhancements are modest.

It is still not possible to reasonably estimate the contribution of direct convective hydration to the tropical lower stratospheric water vapor budget from observations alone. However, the measurements do provide some constraint. Using tropical water vapor profiles saturated with respect to ice up to different cloud-top heights, we show that MLS-retrieved H_2O values at 100 and 82 hPa would not be above the seasonally varying background level unless the convection extended up to about 67/90 hPa during winter/summer months. The lack of enhancements in the tropical MLS H_2O retrievals at 82 and 100 hPa at least indicates that convective hydration up to these pressure levels is either not occurring or produces water vapor plumes that occupy only a fraction of the MLS horizontal footprint.

Another way to look at the problem is to compare the deep tropics with the NAM region. As noted above, there is abundant evidence from both in situ and remote sensing measurements for significant direct convective hydration of the lower stratosphere over North America during the monsoon season, and the regional distribution of lower stratospheric humidity provided by MLS measurements indicates a modest local maximum over the region. The relative lack of clear indications of direct convective hydration in the deep tropics or ASM region suggests that the direct convective impact is much smaller in these regions than over the NAM region.

Satellite-borne lidar (CALIOP) measurements indicated unusually strong convection in the central Pacific during December 2015 associated with the strong 2015–2016 El Niño (Avery et al., 2017). The cloud tops extended above the coincident tropopause height indicated by the MERRA-2 analysis. Cloud-top heights in this convection were the highest observed in the CALIPSO record (Avery et al., 2017), but the Sun-synchronous orbit of the CALIPSO satellite limits measurements to local times near 0130 and 1330, which precludes observations of the strongest continental convection that occurs during late afternoon and early evening. The MLS retrievals in the central Pacific during December 2015 do not indicate any anomalously high H_2O values at 100 or 82 hPa. This null result is consistent with the lack of high MLS H_2O anomalies over regions with comparably deep continental late-afternoon convection that is not sampled by CALIPSO.

Wang et al. (2019) recently used a global-model convective ice water content field, along with trajectory calculations, to evaluate the importance of direct convective hydration for stratospheric water vapor abundance. Their analysis indicated a large convective impact (about 1-ppmv increase in lower stratospheric humidity). The same global-model convective ice product was used by Dessler et al. (2016) to show that convective ice sublimation has an important contribution to model-predicted future trends in stratospheric humidity. The Wang et al. (2019) analysis indicated that the convective hydration in their model was primarily occurring over the ASM, which contradicts the available observational evidence presented here and in previous studies. This inconsistency between the model results and observations attests to the importance of accurately representing the distribution of convective ice relative to the tropopause for estimation of lower stratospheric hydration in models. Convective clouds in most global models, including the one used by Wang et al. (2019), are generated by convective parameterizations, with large uncertainties for even moderately strong convection and even larger uncertainties for the extreme outlier systems reaching the tropopause and beyond.

It is important to reiterate that even if convective clouds do not extend above the local tropopause, the convection may still affect stratospheric humidity indirectly if air parcels hydrated (or dehydrated) by convection in the upper troposphere do not experience cirrus formation on their subsequent journey upward into the stratosphere. Ueyama et al. (2018) showed that the enhanced humidity over the ASM region at 100 hPa (in the upper troposphere) is entirely caused by the frequent convection reaching the uppermost troposphere in the region. Trajectory analyses have shown that air can be effectively transported from the upper

troposphere in the ASM region to the stratosphere (e.g., Yan et al., 2019). This can occur via either isentropic mixing into the extratropical lowermost stratosphere or via ascent into the tropical overworld stratosphere by the Brewer-Dobson circulation. The indirect effect of the ASM convection on stratospheric humidities depends on the relative locations and times of convective hydration and in situ dehydration events.

Data Availability Statement

The MLS water vapor observed by MLS is available from GES DISC (10.5067/Aura/MLS/DATA2009). The NASA airborne measurements of temperature, pressure, and water vapor from the ATTREX and POSIDON campaigns are available at https://espoarchive.nasa.gov/archive/browse/attrex and https://espoarchive.nasa.gov/archive/browse/posidon websites, respectively. The Ticosonde water vapor soundings are available online (at https://acd-ext.gsfc.nasa.gov/Projects/Ticosonde/index.html). (A link to the ftp site is provided under "TICOSONDE Data Access.") The SOWER data can be obtained from the website (http://sower.ees.hokudai.ac.jp/data.html). (Links to bundled data files are provided near the bottom of the page.)

Acknowledgments
Work at the Jet Propulsion Laboratory, California Institute of Technology, was carried out under a contract with NASA.

References

Adler, R. F., & Mack, R. A. (1986). Thunderstorm cloud top dynamics as inferred from satellite observations and a cloud top parcel model. *Journal of the Atmospheric Sciences*, *43*, 1945–1960.

Avery, A. A., Davis, S. M., Rosenlof, K. H., Ye, H., & Dessler, A. E. (2017). Large anomalies in lower stratospheric water vapour and ice during the 2015–2016 El Niño, *10*, 405–409.

Bedka, K. M., & Khlopenkov, K. (2016). A probabilistic multispectral pattern recognition method for detection of overshooting cloud tops using passive satellite Imager observations. *Journal of Applied Meteorology and Climatology*, *55*, 1983–2005.

Bian, J., Pan, L. L., Paulik, L., Vömel, H., Chen, H., & Lu, D. (2012). In situ water vapor and ozone measurements in Lhasa and Kunming during the Asian summer monsoon. *Geophysical Research Letters*, *39*, L19808. https://doi.org/10.1029/2012GL052996

Brewer, A. M. (1949). Evidence for a world circulation provided by the measurements of helium and water vapor distribution in the stratosphere. *Quarterly Journal of the Royal Meteorological Society*, *75*, 351–363.

Connolly, P. J., Vaughan, G., May, P. T., Chemel, C., Allen, G., Choularton, T. W., et al. (2013). Can aerosols influence deep tropical convection? Aerosol indirect effects in the hector island thunderstorm. *Quarterly Journal of the Royal Meteorological Society*, *139*, 2190–2208.

Corti, T., Luo, B. P., de Reus, M., Brunner, D., Cairo, F., Mahoney, M. J., et al. (2008). Unprecedented evidence for deep convection hydrating the tropical stratosphere. *Geophysical Research Letters*, *35*, L10810. https://doi.org/10.1029/2008GL033641

Danielsen, E. F. (1993). In situ evidence of rapid, vertical, irreversible transport of lower tropospheric air into the lower tropical stratosphere by convective cloud turrets and by larger-scale upwelling in tropical cyclones. *Journal of Geophysical Research*, *98*, 8665–8681.

Dauhut, T., Chaboureau, J.-P., Haynes, P. H., & Lane, T. P. (2018). The mechanisms leading to a stratospheric hydration by overshooting convection. *Journal of the Atmospheric Sciences*, *75*, 4383–4398.

Dessler, A. E., Wang, T., Schoeberl, M. R., Oman, L. D., Douglass, A. R., Butler, A. H., et al. (2016). Transport of ice into the stratosphere and the humidification of the stratosphere over the 21st century. *Geophysical Research Letters*, *43*, 2323–2329. https://doi.org/10.1002/2016GL067991

Forster, P. M. F., & Shine, K. P. (2002). Assessing the climate impact of trends in stratospheric water vapor. *Geophysical Research Letters*, *29*(6), 1086. https://doi.org/10.1029/2001GL013909

Fujiwara, M., Vömel, H., Hasebe, F., Shiotani, M., Ogino, S.-Y., Iwasaki, S., et al. (2010). Seasonal to decadal variations of water vapor in the tropical lower stratosphere observed with balloon-borne cryogenic frost point hygrometers. *Journal of Geophysical Research*, *115*, D18304. https://doi.org/10.1029/2010JD014179

Gao, R.-S., Ballard, J., Watts, L. A., Thornberry, T. D., Cliolora, S. J., McLaughlin, R. J., & Fahey, D. W. (2012). A compact, fast UV photometer for measurement of ozone from research aircraft. *Atmospheric Measurement Techniques*, *5*, 2201–2210.

Hall, E. G., Jordan, A. F., Hurst, D. F., Oltmans, S. J., Vömel, H., Kühnreich, B., & Ebert, V. (2016). Advancements, measurement uncertainties, and recent comparisons of the NOAA frost point hygrometer. *Atmospheric Measurement Techniques*, *9*, 4295–4310. https://doi.org/10.5194/amt-9-4295-2016

Hasebe, F., Inai, Y., Shiotani, M., Fujiwara, M., Vömel, H., Nishi, N., et al. (2013). Cold trap dehydration in the tropical tropopause layer characterised by SOWER chilled-mirror hygrometer network data in the tropical Pacific. *Atmospheric Chemistry and Physics*, *13*, 4393–4411. https://doi.org/10.5194/acp-13-4393-2013

Hassim, M. E. E., & Lane, T. P. (2010). A model study on the influence of overshooting convection on TTL water vapor. *Atmospheric Chemistry and Physics*, *10*, 9833–9849.

Hoffmann, L., G, Günther, D, Li, Stein, O., Wu, X., Griessbach, S., et al. (2019). From ERA-Interim to ERA5: The considerable impact of ECMWF's next-generation reanalysis on Lagrangian transport simulations. *Atmospheric Chemistry and Physics*, *19*, 1–2.

Homeyer, C. R., McAuliffe, J. D., & Bedka, K. M. (2017). On the development of above-anvil cirrus plumes in extratropical convection. *Journal of the Atmospheric Sciences*, *74*, 1617–1633.

Hurst, D. F., Oltmans, S. J., Vömel, H., Rosenlof, K. H., Davis, S. M., Ray, E. A., et al. (2011). Stratospheric water vapor trends over Boulder, Colorado: Analysis of the 30 year boulder record. *Journal of Geophysical Research*, *116*, D02306. https://doi.org/10.1029/2010JD015065

Jensen, E. J., Ackerman, A. S., & Smith, J. A. (2007). Can overshooting convection dehydrate the tropical tropopause layer? *Journal of Geophysical Research*, *112*, D11209. https://doi.org/10.1029/2006JD007943

Jensen, E. J., Leonhard, P., Jordan, D. E., Bui, T. V., Ueyama, R., Singh, H. B., et al. (2017). The NASA airborne Tropical TRopopause EXperiment (ATTREX): High-altitude aircraft measurements in the tropical western Pacific. *Bulletin of the American Meteorological Society*, *1*, 129–143. https://doi.org/10.1175/bams-d-14-00263.1

Jensen, E. J., & Pfister, L. (2004). Transport and freeze-drying in the tropical tropopause layer. *Journal of Geophysical Research*, *109*, D02207. https://doi.org/10.1029/2003JD004022

Kelly, K. K., Proffitt, M. H., Chan, K. R., Loewenstein, M., Podolske, J. R., Strahan, S. E., et al. (1993). Water vapor and cloud water measurements over Darwin during the STEP 1987 tropical mission. *Journal of Geophysical Research*, *98*, 8713–8723.

Kley, D., Schmeltekopf, A. L., Kelly, K., Winkler, R. H., Thompson, T. L., & McFarland, M. (1982). Transport of water through the tropical tropopause. *Geophysical Research Letters*, *9*, 617–620.

Krämer, M., Rolf, C., Spelten, N., Afchine, A., Fahey, D., Jensen, E., et al. (2020). A microphysics guide to cirrus—Part II: Climatologies of clouds and humidity from observations. *Atmospheric Chemistry and Physics Discuss*, *20*, 1.

Liu, N., & Liu, C. (2016). Global distribution of deep convection reaching tropopause in 1 year GPM observations. *Journal of Geophysical Research: Atmospheres*, *121*, 3824–3842. https://doi.org/10.1002/2015JD024430

Liu, C., & Zipser, E. J. (2005). Global distribution of convection penetrating the tropical tropopause. *Journal of Geophysical Research*, *110*, D23104. https://doi.org/10.1029/2005JD006063

Meyer, J., Rolf, C., Schiller, C., Rohs, S., Spelten, N., Afchine, A., et al. (2015). Two decades of water vapor measurements with the FISH fluorescence hygrometer: A review. *Atmospheric Chemistry and Physics*, *15*, 8521–8538.

Mote, P. W., Rosenlof, K. H., McIntyre, M. E., Carr, E. S., Gille, J. C., Holton, J. R., et al. (1996). An atmospheric tape recorder: The imprint of tropical tropopause temperatures on stratospheric water vapor. *Journal of Geophysical Research*, *101*, 3989–4006.

Nash, J., Oakley, T., Vömel, H., & Li, W. (2011). WMO intercomparison of high quality radiosonde systems. Retrieved from https://www.wmo.int/pages/prog/www/IMOP/reports/2003-2007/RSO-IC-2005_Final_Report.pdf

Pan, L. L., & Munchak, L. A. (2011). Relationship of cloud top to the tropopause and jet structure from CALIPSO data. *Journal of Geophysical Research*, *116*, D12201. https://doi.org/10.1029/2010JD015462

Randel, W. J., Moyer, E., Park, M., Jensen, E. J., Bernath, P., Walker, K. A., & Boone, C. (2012). Global variations of HDO and HDO/H_2O ratios in the upper troposphere and lower stratosphere derived from ACE-FTS satellite measurements. *Journal of Geophysical Research*, *117*, D06303. https://doi.org/10.1029/2011JD016632

Randel, W. J., & Park, M. (2019). Diagnosing observed stratospheric water vapor relationships to the cold point tropical tropopause. *Journal of Geophysical Research: Atmospheres*, *124*, 7018–7033. https://doi.org/10.1029/2019JD030648

Randel, W. J., Wu, F., Oltmans, S. J., Rosenlof, K., & Nedoluha, G. E. (2004). Interannual changes of stratospheric water vapor and correlations with tropical tropopause temperatures. *Journal of the Atmospheric Sciences*, *61*, 2133–2148.

Read, W. G., Lambert, A., Bacmeister, J., Cofield, R. E., Christensen, L. E., Cuddy, D. T., et al. (2007). Aura Microwave Limb Sounder upper tropospheric and lower stratospheric H_2O and relative humidity with respect to ice validation. *Journal of Geophysical Research*, *112*, D24S35. https://doi.org/10.1029/2007JD008752

Schiller, C., Gross, J.-U., Konopka, P., Plöger, F., dos Santos, F. H. S., & Spelton, N. (2009). Hydration and dehydration at the tropical tropopause. *Atmospheric Chemistry and Physics*, *9*, 9647–9660.

Schoeberl, M., Dessler, A. E., Yee, H., Wang, T., Avery, M. A., & Jensen, E. J. (2016). The impact of gravity waves and cloud nucleation threshold on stratospheric dehydration and tropical tropospheric cloud fraction. *Earth System Science*, *3*, 295–305. https://doi.org/10.1002/2016EA000180

Schoeberl, M. R., Jensen, E. J., Pfister, L., Ueyama, R., Avery, M., & Dessler, A. E. (2018). Convective hydration of the upper troposphere and lower stratosphere. *Journal of Geophysical Research: Atmospheres*, *123*, 4583–4593. https://doi.org/10.1029/2018JD028286

Schoeberl, M. R., Jensen, E. J., Pfister, L., Ueyama, R., Wang, T., Selkirk, H, et al. (2019). Water vapor, clouds, and saturation in the tropical tropopause layer. *Journal of Geophysical Research: Atmospheres*, *124*, 3984–4003. https://doi.org/10.1029/2018JD029849

Schwartz, M. J., Read, W. G., Santee, M. L., Livesey, N. J., Froidevaux, L., Lambert, A., & Manney, G. L. (2013). Convectively injected water vapor in the North American summer lowermost stratosphere. *Geophysical Research Letters*, *40*, 2316–2321. https://doi.org/10.1002/grl.50421

Selkirk, H. B., Vömel, H., Canossa, J. M. V., Pfister, L., Diaz, J. A., Fernandez, W., et al. (2010). Detailed structure of the tropical upper troposphere and lower stratosphere as revealed by balloon sonde observations of water vapor, ozone, temperature, and winds during the NASA TCSP and TC4 campaigns. *Journal of Geophysical Research*, *115*, D00J19. https://doi.org/10.1029/2009JD013209

Smith, J. B., Wilmouth, D. M., Bedka, K. M., Bowman, K. P., Homeyer, C. R., Dykema, J. A., et al. (2017). A case study of convectively sourced water vapor observed in the overworld stratosphere over the United States. *Journal of Geophysical Research: Atmopheres*, *122*, 9529–9554. https://doi.org/10.1002/2017JD026831

Solomon, S., Rosenlof, K., Portmann, R., Daniel, J., Davis, S., Sanford, T., & Plattner, G.-K. (2010). Contributions of stratospheric water vapor changes to decadal variations in the rate of global warming. *Science*, *327*, 1219–1223.

Suzuki, J., Fujiwara, M., Nishizawa, T., Shiroka, R., Yoneyama, K., Katsumata, M., et al. (2013). The occurrence of cirrus clouds associated with eastward propagating equatorial n=0 inertio-gravity and Kelvin waves in November 2011 during the CINDY2011/DYNAMO campaign. *Journal of Geophysical Research: Atmospheres*, *118*, 12,941–12,947. https://doi.org/10.1002/2013JD019960

Tegtmeier, S., Antsey, J., Davis, S., Dragani, R., Harada, Y., Ivanciu, I., et al. (2020). Temperature and tropopause characteristics from reanalyses data in the tropical tropopause layer. *Atmospheric Chemistry and Physics*, *20*, 753–770.

Ueyama, R., Jensen, E. J., & Pfister, L. (2018). Convective influence on the humidity and clouds in the tropical tropopause layer during boreal summer. *Journal of Geophysical Research: Atmospheres*, *123*, 7576–7593. https://doi.org/10.1029/2018JD028674

Ueyama, R., Jensen, E. J., Pfister, L., & Kim, J.-E. (2015). Dynamical, convective, and microphysical control on wintertime distributions of water vapor and clouds in the tropical tropopause layer. *Journal of Geophysical Research: Atmospheres*, *120*, 10,483–10,500. https://doi.org/10.1002/2015JD023318

Vömel, H., Naebert, T., Dirksen, R., & Sommer, M. (2016). An update on the uncertainties of water vapor measurements using cryogenic frost point hygrometers. *Atmospheric Measurement Techniques*, *9*, 3755–3768.

Wang, P. K. (2003). Moisture plumes above thunderstorm anvils and their contributions to cross-tropopause transport of water vapor in midlatitudes. *Journal of Geophysical Research*, *108*(D6), 4194. https://doi.org/10.1029/2002JD002581

Wang, X., Dessler, A. E., Schoeberl, M. R., Yu, W., & Wang, T. (2019). Impact of convectively lofted ice on the seasonal cycle of water vapor in the tropical tropopause layer. *Atmospheric Chemistry and Physics*, *19*, 14,621–14,636.

Yan, X., Konopka, P., Ploeger, F., Podglajen, A., Wright, J. S., Müller, R., & Riese, M. (2019). The efficiency of transport into the stratosphere via the Asian and North American summer monsoon circulations. *Atmospheric Chemistry and Physics*, *19*, 15,629–15,649.

Yang, Q., Fu, Q., & Hu, Y. (2010). Radiative impacts of clouds in the tropical tropopause layer. *Journal of Geophysical Research*, *115*, D00H12. https://doi.org/10.1029/2009JD012393

Zipser, E. J., Cecil, D. J., Liu, C., Nesbit, S. W., & Yorti, D. P. (2006). Where are the most intense thunderstorms on Earth? *Bulletin of the American Meteorological Society*, *87*, 1057–1071.

Zöger, M., Afchine, A., Eicke, N., Gerhards, N., Gerhards, M.-T., Klein, E., et al. (1999). Fast in situ stratospheric hygrometers: A new family of balloonborne and airborne Lyman α photofragment fluorescence hygrometer. *Journal of Geophysical Research*, *104*, 1807–1816.